Proceedings of FEDSM'98
1998 ASME Fluids Engineering Division Summer Meeting
June 21 - 25, 1998, Washington,DC

FEDSM98-4824

CONCEPTUAL ESTIMATE OF POTENTIAL DISTRIBUTIONS IN SPIRAL FLOW BY LEAST NORM METHOD

Masahiro TAKEI
Nihon University, Tokyo Japan

Hui LI
Kagoshima University, Kagoshima Japan

Yao-Hua ZHAO
University of Tokyo, Tokyo Japan

Mitsuaki OCHI
Nihon University, Tokyo Japan

Yoshifuru SAITO
Hosei University, Tokyo Japan

Kiyoshi HORII
Shirayuri Women's College, Tokyo Japan

ABSTRACT
A new concept, that is to estimate inversely two kinds of potential distributions from velocity distribution by means of least norm method on restraint conditions, has been launched. With this concept, the vector potential and the scalar potential of spiral flow has been estimated actually from its velocity distribution. As a result, it makes clear that the spiral flow has the stronger vector potential near the axis. From Helmholtz's theorem, fluid velocity v consists of rotation component from vector potential V and divergent component from scalar potential ϕ as $v = rotV - grad\,\phi$. The estimate of the potentials from the velocity is a ill posed inverse problem. The ill posed inverse problem almost has not been treated in the fluid engineering because a unique solution is not acquired. This study breaks through the drawbacks by means of least norm method on restraint conditions. The least norm method solutions indicate the lowest energy potential, that is the potential of the spiral flow.

KEYWORDS Spiral flow, Swirling flow, Least norm method, Vector potential, Scalar potential

NOMENCLATURE

A	Coefficient matrix of system equation	[m^{-1}]
C	Coefficient matrix between vector potentials **V** and **U**	[-]
$\mathbf{D}_s$	Coefficient matrix between velocity v'' and scalar potential Φ	[m^{-1}]
$\mathbf{D}_v$	Coefficient matrix between velocity v' and vector potential **V**	[m^{-1}]
U	Vector potential matrix of U	[m/s]
U	Vector potential considering restraint condition	[m/s]
V	Vector potential matrix of V	[m^2/s]
V	Vector potential	[m^2/s]
X	Matrix of U and ϕ	[m^2/s]
m	Grid number in x direction	[-]
n	Grid number in y direction	[-]
v	Velocity of spiral flow	[m/s]
v'	Velocity matrix of v'	[m/s]
v'	Velocity caused by vector potential	[m/s]
v''	Velocity matrix of v''	[m/s]
v''	Velocity caused by scalar potential	[m/s]
Φ	Scalar potential matrix of ϕ	[m^2/s]
Ψ	Scalar potential matrix of ϕ	[m^2/s]
ϕ	Scalar potential	[m^2/s]
ϕ	Scalar potential considering restraint condition	[m^2/s]

INTRODUCTION
Spiral flow is useful for industrial applications such as optical cord installation [Horii et al. 1990], dispersion and encapsulation of submicron powders [Horii et al. 1990], high performance transportation [Takei et al. 1997] because the spiral flow has steeper axial velocity and azimuthal velocity with large free vortex region. The motivation behind this work is to clarify the potentials in the spiral flow to improve the performance of the industrial fields. The clarification of the potential is a key point to resolve the mechanism such as swirling motion production and swirling motion continuity for long distance in multiphase spiral flow.
From Helmholtz's theorem, fluid velocity v consists of rotation component from the vector potential V and divergent component from the scalar potential ϕ as $v = rotV - grad\,\phi$. The estimate of the potentials from the velocity is a ill posed inverse problem. The ill posed inverse problem is treated in material engineering [Kubo 1988]. The problem in electro magnetics fields is treated by discrete inverse wavelet transform[Saito 1966]. The ill posed inverse problem almost has not been treated in the fluid engineering because a unique solution is not acquired.
Most of the previous studies in fluid engineering focused on solving the direct problem which is to resolve velocity distribution from the potential distribution. With this idea, the

direct problem to estimate the potential from N-S equation exists[Tokunaga 1991].

The originality of this work lies in the two view points. One is to estimate the unknown potential distributions respectively by resolving the ill posed inverse problem of the system equation. The other is to apply the concept to the estimate of the spiral flow.

In this paper, the new concept, that is to estimate inversely two kinds of potential distributions from velocity distribution by means of least norm method on restraint conditions, has been launched as a first step to resolve the inverse problem. With this concept, the vector potential and the scalar potential of the spiral flow has been estimated actually from its velocity distribution.

CHARACTERISTICS OF SPIRAL FLOW & ITS INVERSE PROBLEM

The nozzle to produce the spiral flow is designed with an annular slit connecting to a conical cylinder as shown in Fig. 1 [Horii 1988]. Pressulized air is forced through the sides of the device into the buffer area, and then through the annular slit into the nozzle outlet. The suction force is generated at the back of the nozzle by Coanda effect. The air, passing through the conical cylinder, develops a spiral structure with a steeper axial velocity and an azimuthal velocity distribution, even if it is not applied tangentially.

The characteristics of the spiral flow has been reported [Horii 1991]. According to the paper, the spiral flow has a steeper axial velocity and an azimuthal velocity with large free vortex region as shown in Figs. 2. In Fig. 2, x axis means the radius of pipe and y axis means the normalized azimuthal velocity. The divergence angle of the spiral flow issued from the nozzle outlet is reduced 45 %, from 14.3 degrees to 7.8 degrees as compared with typical turbulence flow. The turbulent fluctuation level of the spiral flow is decreased about 55%, from 0.20 to 0.09 as compared with that of the typical turbulence flow. These results clearly indicates the focusing characteristic and the high stability of the spiral flow. The particles in the two phase spiral flow obtain high centripetal force. Then, the particles in the spiral flow rotate without touching pipe inner wall as shown in Fig. 3 (a) [Takei et al. 1997]. However, particles in typical turbulence flow collide inside the pipe as shown in Fig. 3 (b). At this experiment, Reynolds number is $1.0X10^5$, the pipe diameter is 62 mm, the specific gravity value of the particles is 3,600 kg/m^3

This paper treats the inverse problem to obtain vector potential and scalar potential from the velocity distribution as shown in Fig. 4 as a first step. The analysis using N-S equation is complicated because the interaction between axial and azimuthal velocities should be considered when the spiral flow generates the swirling motion. The inverse problem is useful for analyzing the spiral flow because the azimuthal velocity is treated directly.

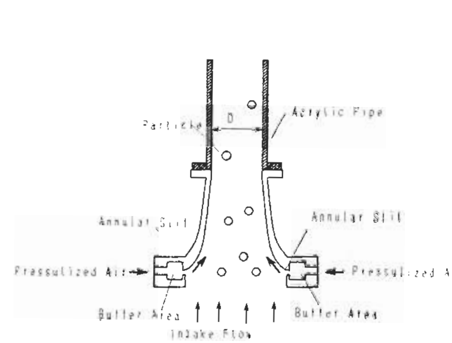

Fig. 1 Nozzle to produce spiral flow

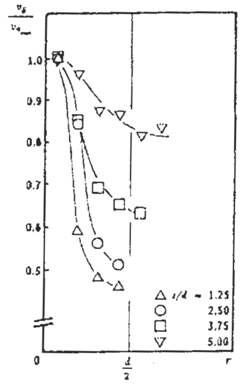

Fig. 2 Azimuthal velocity of spiral flow

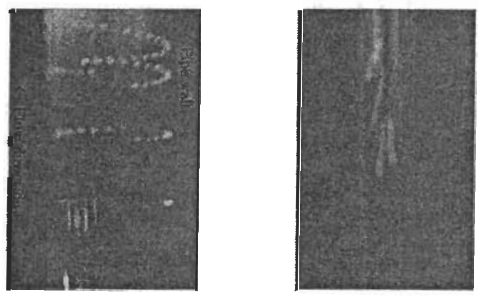

(a) Particles in spiral flow (b) Particles in typical turbulence flow

Fig. 3 Rotating ball in spiral flow

→ **Direct problem** →

N-S Equation	VectorPotential & ScalarPotential	Velocity

← **Inverse problem** ←

Fig. 4 Inverse problem & direct problem

ANALYSIS

Analysis Assumptions & Method

The analysis region is two dimensional cross section in a rectangle pipeline with 2 : 1 ratio between length and height as shown in Fig. 5. The coordinate system for analysis and the flow direction are shown in Fig. 5. The counterclockwise rotation is plus in terms of rotational component. The 16×8 grid is set up on the cross section. Two dimensional vector $\mathbf{v}_1$, $\mathbf{v}_2$ and $\mathbf{v}_3$ are located at each grid as two dimensional air velocities. Values of vector potential $V_1 \sim V_8$ and scalar potential $\phi_1 \sim \phi_8$ are shown distributed on the corners of three adjacent squares (Δx by Δy) of the 16X8 grid to simplify the explanation of the analysis method.

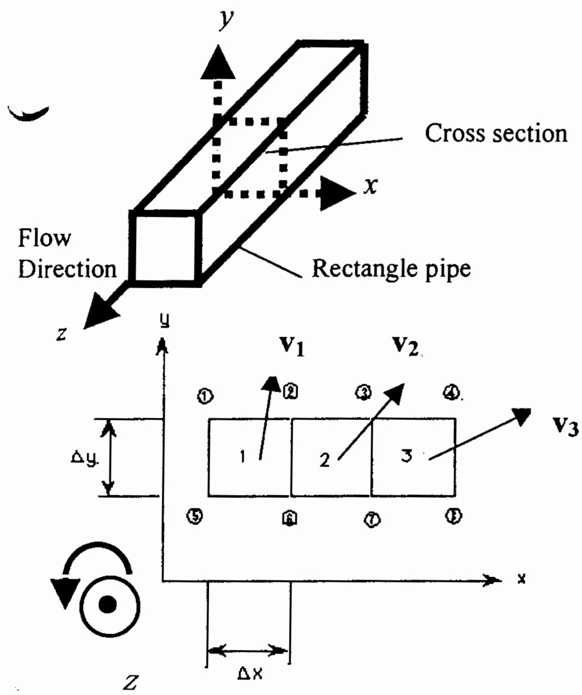

Fig. 5 Coordinate system for analysis

From Helmholtz's theorem, a velocity vector **v** consists of a rotational component from the vector potential **V** and a divergent component from the scalar potential ϕ as,

$$\mathbf{v} = rot\mathbf{V} - grad\phi \qquad (1)$$

Vector potential is also called stream function. Scalar potential is also called velocity potential. Firstly, the relation between the velocity vector **v'** from the vector potential and the vector potential **V** is obtained. The velocity vector **v'** from the vector potential is expressed by

$$\mathbf{v}' = rot\mathbf{V} = \left(\frac{\partial V_z}{\partial y}\right)\mathbf{i} - \left(\frac{\partial V_z}{\partial x}\right)\mathbf{j} \qquad (2)$$

Where V_z is a vector potential in z direction on the cross section, **i** and **j** are unit vectors in x and y directions, respectively.

The Eq. (2) is rewritten by central difference and matrix expression as

$$\begin{bmatrix} v'_{1x} \\ v'_{2x} \\ v'_{3x} \\ v'_{1y} \\ v'_{2y} \\ v'_{3y} \end{bmatrix} = \frac{1}{2}\begin{bmatrix} \frac{1}{\Delta y} & \frac{1}{\Delta y} & 0 & 0 & -\frac{1}{\Delta y} & -\frac{1}{\Delta y} & 0 & 0 \\ 0 & \frac{1}{\Delta y} & \frac{1}{\Delta y} & 0 & 0 & -\frac{1}{\Delta y} & -\frac{1}{\Delta y} & 0 \\ 0 & 0 & \frac{1}{\Delta y} & \frac{1}{\Delta y} & 0 & 0 & -\frac{1}{\Delta y} & -\frac{1}{\Delta y} \\ \frac{1}{\Delta x} & -\frac{1}{\Delta x} & 0 & 0 & \frac{1}{\Delta x} & -\frac{1}{\Delta x} & 0 & 0 \\ 0 & \frac{1}{\Delta x} & -\frac{1}{\Delta x} & 0 & 0 & \frac{1}{\Delta x} & -\frac{1}{\Delta x} & 0 \\ 0 & 0 & \frac{1}{\Delta x} & -\frac{1}{\Delta x} & 0 & 0 & \frac{1}{\Delta x} & -\frac{1}{\Delta x} \end{bmatrix}\begin{bmatrix} V_1 \\ V_2 \\ V_3 \\ V_4 \\ V_5 \\ V_6 \\ V_7 \\ V_8 \end{bmatrix}$$

$$\mathbf{v}' = \mathbf{D_V V} \qquad (3)$$

In this equation, the number of V is larger than that of v'. A restraint condition in terms of Eq. (3), the amount of vector potential magnitude are zero, is set up as

$$\sum_{i=1}^{8} V_i = 0 \qquad (4)$$

From Eq. (4), using a matrix **U**, the vector potential **V** is expressed by

$$\begin{bmatrix} V_1 \\ V_2 \\ V_3 \\ V_4 \\ V_5 \\ V_6 \\ V_7 \\ V_8 \end{bmatrix} = \begin{bmatrix} 1 & 0 & 0 & 0 & 0 & 0 & 0 \\ 0 & 1 & 0 & 0 & 0 & 0 & 0 \\ 0 & 0 & 1 & 0 & 0 & 0 & 0 \\ 0 & 0 & 0 & 1 & 0 & 0 & 0 \\ 0 & 0 & 0 & 0 & 1 & 0 & 0 \\ 0 & 0 & 0 & 0 & 0 & 1 & 0 \\ 0 & 0 & 0 & 0 & 0 & 0 & 1 \\ -1 & -1 & -1 & -1 & -1 & -1 & -1 \end{bmatrix}\begin{bmatrix} U_1 \\ U_2 \\ U_3 \\ U_4 \\ U_5 \\ U_6 \\ U_7 \end{bmatrix}$$

$$\mathbf{V} = \mathbf{CU} \qquad (5)$$

Next, the relation between the velocity vector **v''** from the scalar potential and the scalar potential ϕ is obtained. The velocity vector **v''** from the scalar potential is expressed by

$$\begin{bmatrix} v''_{1x} \\ v''_{2x} \\ v''_{3x} \\ v''_{1y} \\ v''_{2y} \\ v''_{3y} \end{bmatrix} = \frac{1}{2}\begin{bmatrix} \frac{1}{\Delta x} & \frac{1}{\Delta x} & 0 & 0 & -\frac{1}{\Delta x} & -\frac{1}{\Delta x} & 0 & 0 \\ 0 & \frac{1}{\Delta x} & \frac{1}{\Delta x} & 0 & 0 & -\frac{1}{\Delta x} & -\frac{1}{\Delta x} & 0 \\ 0 & 0 & \frac{1}{\Delta x} & \frac{1}{\Delta x} & 0 & 0 & -\frac{1}{\Delta x} & -\frac{1}{\Delta x} \\ \frac{1}{\Delta y} & -\frac{1}{\Delta y} & 0 & 0 & \frac{1}{\Delta y} & -\frac{1}{\Delta y} & 0 & 0 \\ 0 & \frac{1}{\Delta y} & -\frac{1}{\Delta y} & 0 & 0 & \frac{1}{\Delta y} & -\frac{1}{\Delta y} & 0 \\ 0 & 0 & \frac{1}{\Delta y} & -\frac{1}{\Delta y} & 0 & 0 & \frac{1}{\Delta y} & -\frac{1}{\Delta y} \end{bmatrix}\begin{bmatrix} \phi_1 \\ \phi_2 \\ \phi_3 \\ \phi_4 \\ \phi_5 \\ \phi_6 \\ \phi_7 \\ \phi_8 \end{bmatrix}$$

$$\mathbf{v}'' = \mathbf{D_S}\boldsymbol{\Phi} \qquad (6)$$

In this equation, the number of ϕ is larger than that of v''. A restraint condition in terms of Eq. (6) is considered as

$$\sum_{i=1}^{8} \phi_i = 0 \qquad (7)$$

From Eq. (7), using a potential matrix $\boldsymbol{\Psi}$, the scalar potential $\boldsymbol{\Phi}$ is

$$
\begin{bmatrix}\phi_1\\ \phi_2\\ \phi_3\\ \phi_4\\ \phi_5\\ \phi_6\\ \phi_7\\ \phi_8\end{bmatrix}=\begin{bmatrix}1&0&0&0&0&0&0\\0&1&0&0&0&0&0\\0&0&1&0&0&0&0\\0&0&0&1&0&0&0\\0&0&0&0&1&0&0\\0&0&0&0&0&1&0\\0&0&0&0&0&0&1\\-1&-1&-1&-1&-1&-1&-1\end{bmatrix}\begin{bmatrix}\varphi_1\\ \varphi_2\\ \varphi_3\\ \varphi_4\\ \varphi_5\\ \varphi_6\\ \varphi_7\end{bmatrix}
$$

$$\mathbf{\Phi} = \mathbf{C\Psi} \qquad \text{——(8)}$$

From Eqs. (3), (5), (6) and (8), the system equation between the potential and the velocity is

$$\mathbf{v} = \mathbf{D_v V} + \mathbf{D_S \Phi} = \left[\mathbf{D_v C} + \mathbf{D_S C}\right]\begin{bmatrix}\mathbf{U}\\ \mathbf{\Psi}\end{bmatrix} = \mathbf{AX} \qquad \text{——(9)}$$

A is a coefficient matrix of the system equation as $\mathbf{A} = \mathbf{D_v C} + \mathbf{D_s C}$. In this analysis, $\Delta x = \Delta y = 1.0$ is assumed.

Two Dimensional Velocity Model of Spiral Flow

From Figs. 2 and 3, the spiral flow has azimuthal velocity with large free vortex region. Two types of two dimensional model of spiral flow are analyzed. One with mean velocity is assumed as

$$v_{ij} = \left(\sin\left[\frac{2\pi i}{m}\right] \bullet v_x, \sin\left[\frac{2\pi j}{n}\right] \bullet v_y\right) \quad \text{[m/s]} \qquad \text{——(10)}$$

Where, v_x and $v_y = 1.0$[m/s], i and j are grid numbers in x and y directions. Eq. (10) draws the velocity distribution in Fig. 6. The highest azimuthal velocity is 1.0 m/s and the lowest azimuthal velocity is 0.0 m/s. Flow pattern of typical turbulence flow in a rectangle pipe is experienced. Eddy occurs at four corners, resulting in divergence velocity component. In this analysis, not only rotation component but also divergence component are considered in order to compare the analysis result easily as a preliminary study. The grid number in x and y directions are m=16, n=8 respectively.

The other model with random fluctuation from –0.3[m/s] to +0.3[m/s] is set up as

$$vf_{ij} = \left(\sin\left[\frac{2\pi i}{m}\right] \bullet v_x + vf', \sin\left[\frac{2\pi j}{n}\right] \bullet v_y + vf'\right) \quad \text{[m/s]} \qquad \text{——(11)}$$

Eq. (11) draws the velocity distribution in Fig. 7. vf' is random fluctuation.

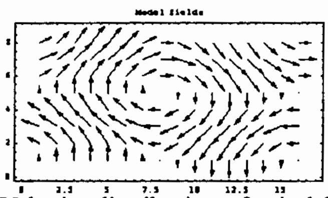

Fig. 6 Velocity distribution of spiral flow

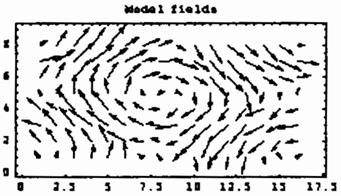

Fig. 7 Velocity distribution with fluctuation

Least Norm Analysis of Ill Posed Inverse Problem

The way to obtain the vector potential **V** and the scalar potential $\mathbf{\Phi}$ from the velocity **v** is to resolve the ill posed problem because the equation number is 256 and the unknown number is 306 in Eq. (9). This paper applies the least norm method to acquiring the approximate resolution. Least norm resolution with regard to Eq. (9) is expressed by

$$\mathbf{X} = \begin{bmatrix}\mathbf{U}\\ \mathbf{\Psi}\end{bmatrix} = \mathbf{A}^{\mathrm{T}}\left(\mathbf{A} \bullet \mathbf{A}^{\mathrm{T}}\right)^{-1}\mathbf{v} \qquad \text{——(12)}$$

The coefficient matrix on the right term in Eq. (12) is an inverse matrix of **A** in Eq. (9). The norm of **X** is square root of square sum of each element as shown in

$$\|\mathbf{X}\| = \sqrt{U_1^{\,2} + U_2^{\,2} + U_3^{\,2} + \bullet\bullet\bullet \varphi_1^{\,2} + \varphi_2^{\,2} + \varphi_3^{\,2} + \bullet\bullet\bullet} \qquad \text{——(13)}$$

Each element resolution by least norm method shows the value when the norm is the lowest. That is assumed to be a potential of spiral flow.

Fig. 8 shows the vector potential **V** (a) and its velocity distribution **v'** (b). Fig. 8 (a) indicates the contour map whose darker part is a smaller value, and whiter part is a larger value. The maximum potential is 1.765[m^2/s], the minimum is –3.075[m^2/s]. Fig. 8 (b) is obtained from Eq. (3). Fig. 9 shows the scalar potential $\mathbf{\Phi}$ (a) and its velocity **v''** (b). Fig. 9 (a) shows the contour map whose maximum potential is 2.086[m^2/s], the minimum is –2.062[m^2/s]. Fig. 9 (b) is obtained from Eq. (6). Adding the velocity vectors from the vector potential and the scalar potential is completely the same as the model velocity in Fig. 6.

From Fig. 8 (a), the center of the potential contour is minimum in counterclockwise rotation, that is maximum in clockwise rotation. The potential value is decreased in proportion to going outside. The spiral flow has the stronger vector potential near the axis. From Fig. 8(b), it is possible to estimate the direction and length of the velocity vector.

From Fig. 9 (b), the velocity at the four corner is the same as the divergence direction in Fig. 6. At the upper left in Fig. 9 (b), the velocity from scalar potential indicates the opposite direction against the model velocity in Fig. 6. Because the model velocity decreases in proportion to x at the part, the opposite direction of the scalar velocity is reasonable.

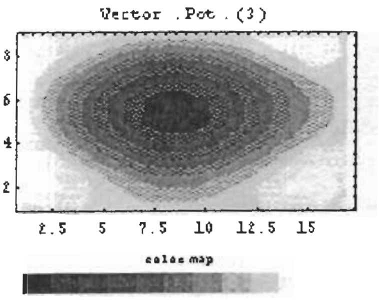

(a) Contour of vector potential

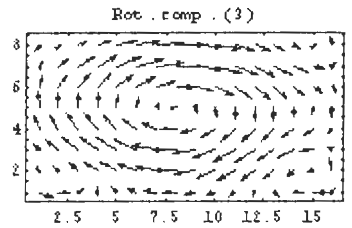

(b) Velocity distribution from vector potential

Fig. 8 Vector potential and its velocity distribution

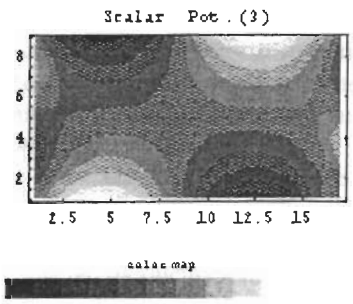

(a) Contour of scalar potential

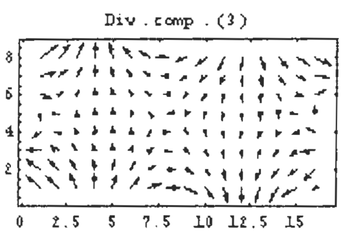

(b) Velocity distribution from scalar potential

Fig. 9 Scalar potential and its velocity distribution

Analysis of Spiral Flow with Fluctuation

The model in Fig. 7 is analyzed by Eq. (12). Fig. 10 shows the vector potential **V** (a) and its velocity distribution **v'** (b). The maximum potential is 2.022[m^2/s] and the minimum is –3.194[m^2/s] in Fig. 10 (a).

Fig. 11 shows the scalar potential Φ (a) and its velocity distribution **v''** (b). In Fig. 11 (a), the maximum potential is 2.319[m^2/s] and minimum is –2.135[m^2/s]. Adding the velocity vectors from the vector potential and the scalar potential is completely the same as the model velocity in Fig. 7. From these figures, even though the model includes the fluctuation, the potentials and their velocities can be extracted clearly.

To discuss the results, a mean velocity difference between the original velocity v_{ij} and the velocity with fluctuation vf_{ij} at each grid is defined as

$$v_m = \frac{1}{m \bullet n}\left(\sum_{j=1}^{n}\sum_{i=1}^{m}\left(v_{ij} - vf_{ij}\right)\right) \qquad \text{——(14)}$$

Substituting v_{ij} and vf_{ij} at each grid in Figs. 8 (b) and 10 (b) for Eq. (14), the mean difference of the vector potential velocity can be obtained as 0.1246. On the other hand, substituting v_{ij} and vf_{ij} at each grid in Figs. 9 (b) and 11 (b) for Eq. (14), the mean difference of the scalar potential velocity can be obtained as 0.1429. From these results, the vector potential velocity is less affected by the fluctuation than the scalar potential velocity because the fluctuation is random value that is scalar value.

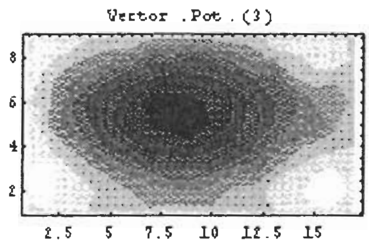

(a) Contour of vector potential

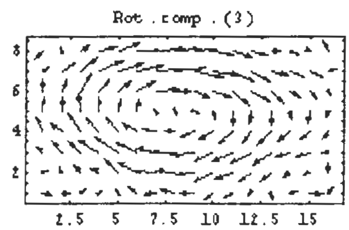

(b) Velocity distribution from vector potential

Fig. 10 Vector potential and its velocity distribution

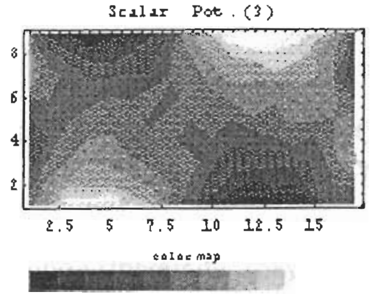

(a) Contour of scalar potential

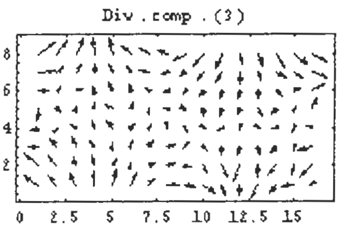

(b) Velocity distribution from scalar potential

Fig. 11 Scalar potential and its velocity distribution

CONCLUSIONS

A new concept, that is to estimate inversely two kinds of potential distributions from velocity distribution by means of least norm method on restraint conditions, has been launched. With this concept, the vector potential and the scalar potential of the spiral flow has been estimated actually from its velocity distribution. As a result, (1) It is possible to extract each potential and its velocity. (2) It makes clear that the spiral flow has the stronger vector potential near the axis. (3) The vector potential is less affected by fluctuation than the scalar potential.

ACKNOWLEDGMENTS

This study is supported by Mikiya Science and Technology Foundation in Japan.

REFERENCES

Horii,K., (1988) *US.PAT. No.4,721,126, UK.PAT.* No.2, 180, 957.

Horii,K., (1990) Using Spiral Flow for Optical Cord Passing *Mechanical Engineering - ASME*, Vol.112, No.8, pp68-69

Horii,K. et al., (1990) New Continuous System For Dispersion and Encapsulation of Submicron Powder Using Spiral Flow, *ASME FED-Vol.00, Industrial Applications of Fluid Mechanics*, pp25-30.

Horii,K. et al., (1991) A Coanda Spiral Device Passing Optical Cords with Mechanical Connectors Attached through a Pipeline, *ASME FED-Vol.121, Gas-Solid Flows*, pp65-70.

Kubo,S., (1988) Inverse Problem Related to the Mechanics and Fracture of Solids and Structures, *JSME Int. J. Ser.I*, Vol.31, No.2, pp157-166

Saito,Y., (1996) Wavelet Analysis for Computational Electromagnetics, (in Japanese), *Trans. IEE of Japan*, Vol. 116A, No10, pp833-839

Takei,M.et al., (1997) Transporting Particles without Touching Pipe Wall, *ASME FED*, FEDSM97-3629

Tokunaga,H. et al.(1991), Direct Simulations of Three-Dimensional Flows Using Generalized Vector Potential Method *AIAA Paper*91-1610, pp937-946(1991)